Available online at www.sciencedirect.com

ScienceDirect

International Journal of Thermal Sciences 48 (2009) 837–846

International Journal of Thermal Sciences

www.elsevier.com/locate/ijts

Isothermal and non-isothermal crystallization kinetics of modified rape straw flour/high-density polyethylene composites

Peng Zou, Shangwen Tang, Zizheng Fu, Hanguo Xiong *

College of Food Science and Technology, Huangzhong Agricultural University, Wuhan 430070, China

Received 20 November 2007; received in revised form 19 May 2008; accepted 16 June 2008

Abstract

The isothermal and non-isothermal crystallization kinetics of modified rape straw flour/high-density polyethylene (MRSF/HDPE) composites were investigated by means of differential scanning calorimetry (DSC). The Avrami model was applied to describe the process of isothermal crystallization. According to Hoffman–Weeks theory, the values of the equilibrium melting point (T_m^0) increased with an increase in the content of MSRF in the composites. The nucleation constant K_g was obtained through the use of the Hoffman and Lauritzen theory. Several theoretical models were applied to describe the process of non-isothermal crystallization. The results showed that the Avrami analysis modified by Jeziorny and a method developed by Mo could describe the non-isothermal crystallization of the composites very well. However, the Ozawa analysis did not give an adequate description. Kinetic parameters such as the Avrami exponent (n), the kinetic crystallization rate constant (Z_c), the peak temperatures (T_{peak}), the half-time of crystallization ($t_{1/2}$), and the like were determined at various scanning rates.

Keywords: Rape straw flour; HDPE; Isothermal crystallization; Non-isothermal crystallization; Kinetics; DSC

1. Introduction

High-density polyethylene (HDPE) is currently the most widely used commercial polymer due to its superior mechanical and physical properties. However, its toughness, weather resistance, processability, and environmental stress cracking resistance are not good enough, which have thus limited its application in many high-technology fields. Reinforcing it with some fillers to form a composite has been found to be one measure to improve its properties [1–3].

Wood fiber plastic composites (WPCs) have gained significant popularity in the last decade [4–7]. However, there have been few recent investigations on rape straw flour/high-density polyethylene composites as WPCs. When rape straw flour is added to plastics, stiffness is enhanced which is an advantage in certain areas of use. When proper coupling agents are used to improve fiber-matrix adhesion, rape straw flour can also be used to reinforce the plastic. There are also economical and environmental reasons for replacing part of the plastic with rape straw flour.

The crystallization behavior of polymer is a basic problem in polymer physics. Particularly, the filler in a polymer will affect extensively the crystallization behavior of the polymer-based composites [8]. Crystallization of polymers is usually studied by the DSC method. The crystallization process can proceed under either isothermal condition or non-isothermal conditions. From the practical view, the non-isothermal crystallization is more useful than the isothermal crystallization. There are many papers on studying the crystallization kinetics of polyethylenes or polyethylene composites [9–12]. Zheng et al. [13] investigated the crystallization behavior of rare earth neodymium-iron-boron (NdFeB) magnetic powder/high density polyethylene composite. The results showed there was a remarkable heterogeneous nucleation effect of NdFeB on the HDPE matrix. Run et al. [14] reported non-isothermal crystallization kinetics of ternary blends of the mPE/LDPE/LLDPE using DSC at various scanning rates. The results speak that Mo method is successful in describing the non-isothermal crystallization process of mPE/LLDPE/LDPE ternary blends, while Ozawa theory is not accurate to interpret the whole process of

---

* Corresponding author. Tel.: +86 2763 215853; fax: +86 2787 286608.
E-mail address: xionghanguo@163.com (H. Xiong).

doi:10.1016/j.ijthermalsci.2008.06.010

nonisothermal crystallization. But few publications have been found concerning the crystallization kinetics of WPCs, especially rape straw flour/high-density polyethylene composites. In this paper, the isothermal and non-isothermal crystallization kinetics of HDPE and MRSF/HDPE composites are investigated. From DSC measurements, a study on isothermal crystallization kinetics is performed using the Avrami theory, and the crystallization activation energy is also calculated using the Hoffman and Lauritzen theory. It is well known that polymer and composites usually undergo a non-isothermal crystallization process, especially in practical processing. The investigation of crystallization behavior can serve to guide the process and application. T_{onset} is relevant to industrial processing so it is thus desirable to study the crystallization of MRSF/HDPE composites under non-isothermal conditions. This is especially important because isothermal crystallization conditions are rarely met during practical processing. In our study, several theoretical models were applied to describe the process of non-isothermal crystallization.

2. Experimental method

2.1. Materials

Rape straw flour (RSF) with a size of 74 µm was provided by the National Engineering Research Center of Rapeseed, China. It was first dried in 170 °C for 24 hours, then the surface of RSF was modified by a silane coupling agent (SG-Si900) (RSF/SG-Si900 100/2 by weight) which was purchased from Nanjing Shuguang Chemical Co. before use. Meanwhile, HDPE (5000 s) which was used without any treatment and has a melt index of 0.7 g/10 min is a product of Daqing Petrochemical Co.

2.2. Preparation of the MRSF/HDPE composites

The HDPE and rape straw flour modified with a silane coupling agent were mixed in a roller at 145–150 °C for 15–20 min. The resulting sheet was compression molded at 170 °C into a 1 mm-thick sheet under a pressure of 9 MPa for 15 min and then was kept at room temperature. The ratios of HDPE/modified rape straw flour (MRSF) particle are 100/0, 100/20, 100/40, 100/60, 100/80, and 100/100 according to weight, respectively.

2.3. Thermal measurements

The isothermal and non-isothermal crystallization kinetics of MRSF/HDPE composites was carried out on a Nexus DSC 204F1 in nitrogen atmosphere. The temperature and melting enthalpy were calibrated with standard indium at each cooling rate in the measurement. As to the isothermal crystallization kinetics, the samples of 5–10 mg were encapsulated into aluminum pans and were rapidly heated at a rate of 40 °C/min to 170 °C above the melting temperature. They stayed there for 1 min to eliminate any residual crystals, and then were rapidly cooled to the designated crystallization temperature (T_c) at a rate of 40 °C/min. The three different temperatures were in the range of 120–122 °C for each sample in the isothermal crystallization process. After which, the samples were held at their designated temperature for 10 min until crystallization was complete. The specimens were subsequently heated to 170 °C at a rate of 10 °C/min. As to the non-isothermal crystallization kinetics, the samples of 5–10 mg were encapsulated into aluminum pans and were heated first up to 170 °C rapidly from 50 °C, and this temperature was maintained for 5 min in order to eliminate the thermal history of the samples. Then the samples were cooled down to 50 °C at four different cooling rates of 2.5, 5, 10 and 15 °C /min, respectively.

2.4. Polarized optical microscopy (POM) measurements

The spherulite growth process and the developed crystal morphology were observed on an Olympus polarized optical microscopy (POM) with BX51 M system, which is equipped with a Mettler Toledo FP82HT hot stage and a Mettler Toledo FP90 controller. The samples were firstly melted between two glass slides at 200 °C for 10 min in a hot stage and then transferred fleetly into another hot stage in the microscopy, which was preheated and kept at 123 °C. The digital images of crystallization process were recorded with the integrating BX51 M video camera system.

3. Results and discussion

3.1. Isothermal crystallization kinetics of MRSF/HDPE composites

3.1.1. Isothermal crystallization behavior of the HDPE and MRSF/HDPE composites

The isothermal thermograms of the HDPE and MRSF/HDPE composites obtained by cooling a molten polymer to the crystallization temperature (T_c) are shown in Fig. 1. It can be seen that the crystallization of HDPE is strongly affected by T_c. With an increase in T_c, the exothermic peaks shifted to a higher value, the crystallization exothermic peak became flatter, and the time to reach the maximum degree of crystallization increased. This indicates that the crystallization rate decreases with an increase in T_c. The influence of crystallization temperature on crystallization is similar for both the HDPE and MRSF/HDPE composites. However, adding MRSF prolongs the time to reach the half degree of crystallization shown in Table 1, indicating a decrease in crystallization rate. This implies that the MRSF cannot act as a nucleating agent for the HDPE matrix, and a large MRSF size can lessen the adsorption of MRSF to the HDPE chain due to steric hindrance.

The relative degree of crystallinity (X_t) is obtained from the area of the exothermic peak of isothermal crystallization analysis in DSC. X_t is a function of time, which is plotted in Fig. 2. It can be seen that all of the curves have the same "S" shape. Furthermore, characteristic sigmoid isotherms shift to the right with an increase in isothermal crystallization temperature, and the crystallization rate becomes slower.

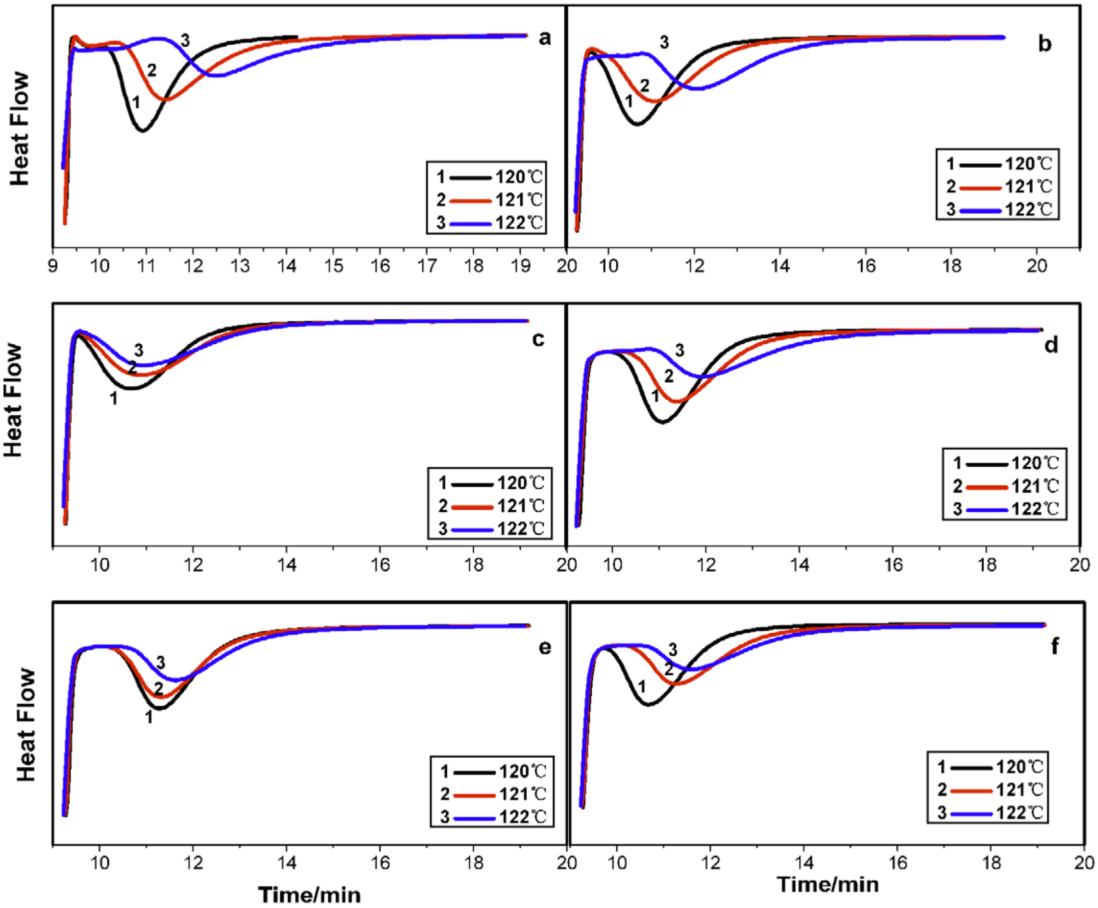

Fig. 1. The DSC traces of samples isothermally crystallized at the specified temperature: (a) HDPE:MRSF = 100:0; (b) HDPE:MRSF = 100:20; (c) HDPE:MRSF = 100:40; (d) HDPE:MRSF = 100:60; (e) HDPE:MRSF = 100:80; (f) HDPE:MRSF = 100:100 (by weight).

Table 1
Avrami kinetic parameters from the Avrami equation for the isothermal crystallization of samples

Samples	T_c (°C)	$t_{1/2}$ (s)	n	K (min^{-1})
HDPE/MRSF (100/0 w/w)	120	38.2	2.4	1.21
	121	60.6	2.3	0.67
	122	68.2	2.3	0.52
HDPE/MRSF (100/20 w/w)	120	65.3	2.6	0.57
	121	76.9	2.7	0.27
	122	86.0	2.2	0.42
HDPE/MRSF (100/40 w/w)	120	76.6	2.8	0.36
	121	91.8	2.9	0.20
	122	95.4	2.7	0.20
HDPE/MRSF (100/60 w/w)	120	51.4	2.3	1.00
	121	57.0	2.3	0.79
	122	68.1	2.2	0.54
HDPE/MRSF (100/80 w/w)	120	51.5	2.3	1.01
	121	55.9	2.3	0.82
	122	65.2	2.4	0.58
HDPE/MRSF (100/100 w/w)	120	62.2	2.6	0.63
	121	62.8	2.3	0.63
	122	68.1	2.2	0.53

Generally, the analysis of the isothermal crystallization kinetics of polymers and polymer composites was performed using the classical Avrami equation [15–17] as given in Eq. (1)

$$1 - X_t = \exp(-Kt^n) \tag{1}$$

where the K and n values denote the crystallization rate constant and the Avrami exponent, respectively. Both K and n depend on the nucleation and growth mechanisms of spherulites. X_t is the relative crystallinity of the polymers at different temperatures or time, t is the time taken during the crystallization process.

In order to deal conveniently with the operation, Eq. (1) is usually rewritten as a double logarithmic form as follows:

$$\ln\bigl[-\ln(1 - X_t)\bigr] = \ln K + n \ln t \tag{2}$$

Plotting $\ln[-\ln(1 - X_t)]$ versus $\ln t$ for each cooling rate as shown in Fig. 3, it can be seen that each curve shows an almost linear relationship. This indicates that the Avrami equation can properly describe the isothermal crystallization behavior of the samples. From the slope and intercept of the lines, the Avrami exponent n and the crystallization rate K can be determined. Meanwhile, the crystallization half-time $t_{1/2}$ is defined as the time at which the extent of crystallization is 50%.

The Avrami exponent n, the crystallization rate K, and the crystallization half-time $t_{1/2}$ at different crystallization temperatures are listed in Table 1. In the Avrami expression, the Avrami exponent n provides qualitative information on the nature of nucleation and the growth processes. The n values of MRSF/HDPE composites are roughly larger than those of neat HDPE at the same T_c (Table 1). The values of K, which is re-

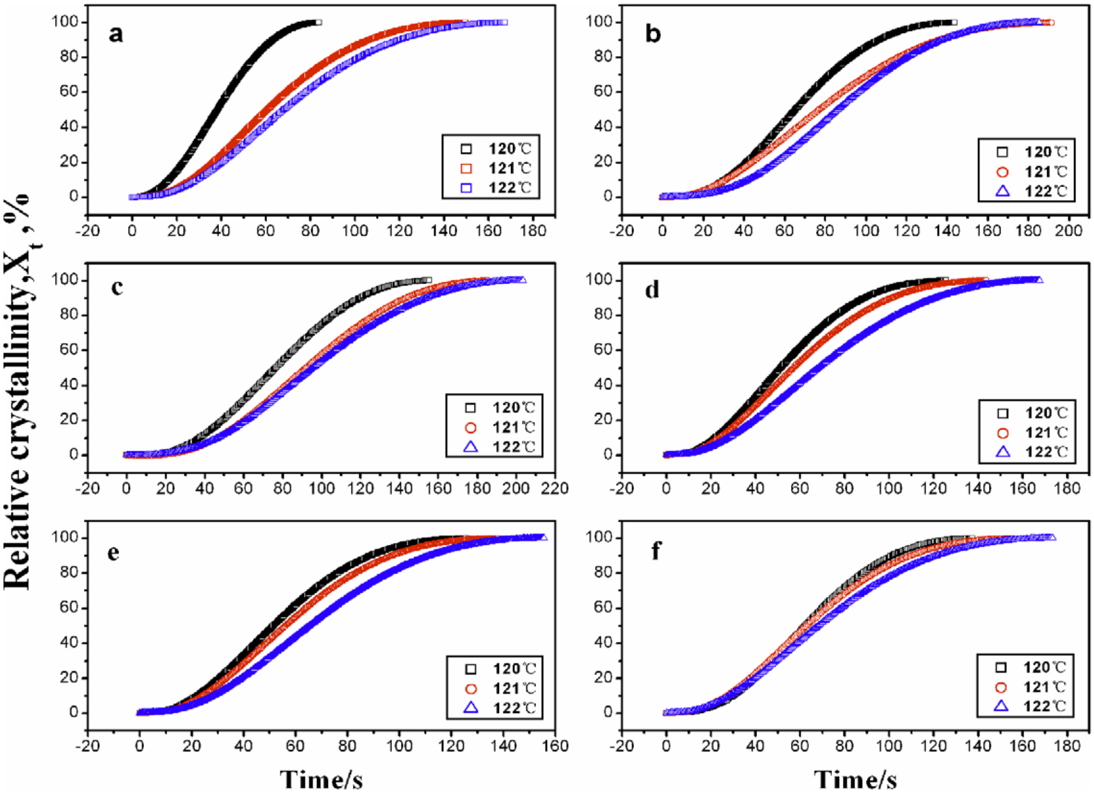

Fig. 2. Plots of X_t versus t for the isothermal crystallization of samples at the specified temperature: (a) HDPE:MRSF = 100:0; (b) HDPE:MRSF = 100:20; (c) HDPE:MRSF = 100:40; (d) HDPE:MRSF = 100:60; (e) HDPE:MRSF = 100:80; (f) HDPE:MRSF = 100:100 (by weight).

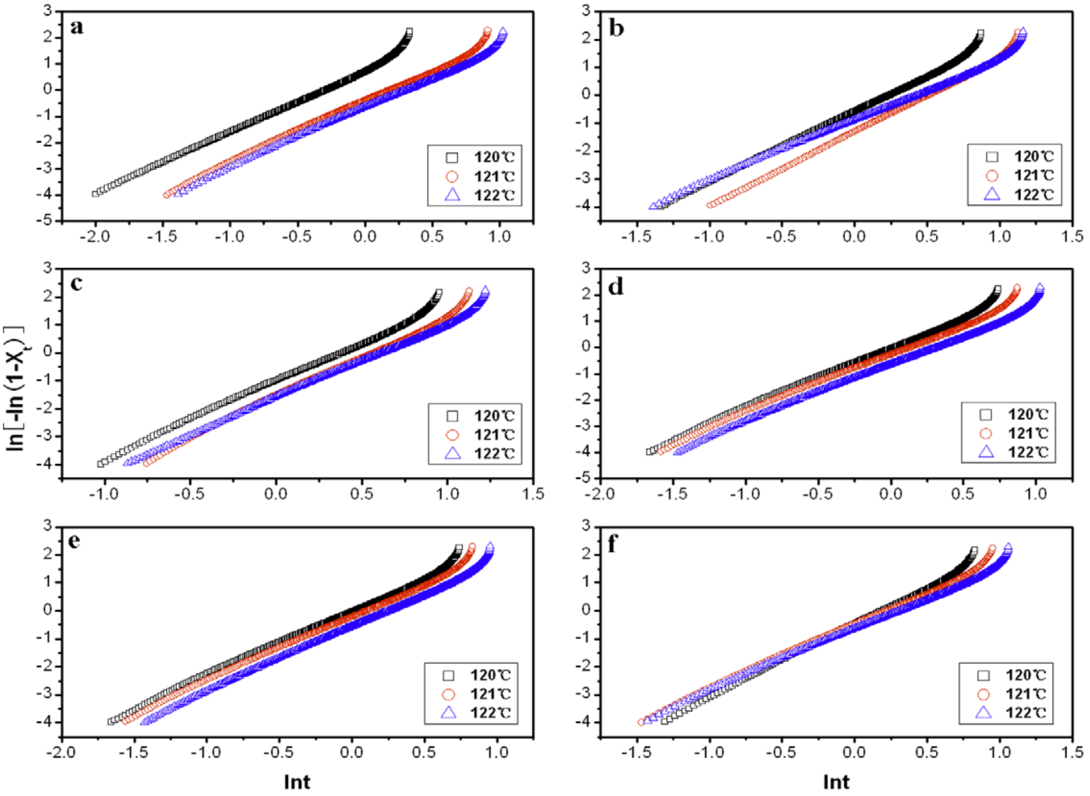

Fig. 3. Plots of $\ln[-\ln(1 - X_t)]$ versus $\ln t$ for the isothermal crystallization of samples at the specified temperature: (a) HDPE:MRSF = 100:0; (b) HDPE:MRSF = 100:20; (c) HDPE:MRSF = 100:40; (d) HDPE:MRSF = 100:60; (e) HDPE:MRSF = 100:80; (f) HDPE:MRSF = 100:100 (by weight).

Table 2
Values of T_m^0, K_g and σ at various T_c for HDPE and MRSF/HDPE composites

Samples	T_m^0 (K)	K_g (K^2)	σ (J/m^2)
HDPE/MRSF (100/0 w/w)	413.9	3.006×10^5	1.903×10^{-2}
HDPE/MRSF (100/20 w/w)	420.4	1.502×10^5	9.361×10^{-3}
HDPE/MRSF (100/40 w/w)	422.0	1.224×10^5	7.602×10^{-3}
HDPE/MRSF (100/60 w/w)	423.8	1.529×10^5	9.456×10^{-3}
HDPE/MRSF (100/80 w/w)	426.6	1.303×10^5	8.006×10^{-3}
HDPE/MRSF (100/100 w/w)	426.5	5.961×10^4	3.663×10^{-3}

lated to nucleation rate and growth processes, decreased with an increase in T_c in all the cases (Table 1). The incorporation of MRSF significantly increased the crystallization kinetic constant K, suggesting that MRSF cannot act as effective nucleating agents and decelerate the crystallization of HDPE in the composites. Generally, $t_{1/2}$ is used to characterize the crystallization rate. The longer the $t_{1/2}$, the slower the crystallization rate. In all samples, $t_{1/2}$ increases with an increase in T_c. The $t_{1/2}$ values of the composites are higher than those of neat HDPE. This implies that MRSF decelerates the crystallization of HDPE in the composites, which is in accordance with the above result.

3.1.2. Equilibrium melting point (T_m^0)

To carry on with the quantitative analysis of crystallization behavior, especially to investigate the temperature dependence of crystallization rate, it is necessary to determine the equilibrium melting point as accurately as possible. The reliable estimation of the equilibrium melting point can be made by careful DSC studies. According to the Hoffman–Weeks theory [18], the equilibrium melting point may be deduced by plotting the observed apparent melting temperature (T_m) against the crystallization temperature (T_c). The equilibrium melting point is obtained by an extrapolation of the resulting straight line to intersect the line $T_m = T_c$. The values of T_m^0 are listed in Table 2. As is shown in the table, the values of T_m^0 increase with an increase in content of MSRF in the composites.

3.1.3. Hoffman and Lauritzen theory

From the isothermal crystallization, the growth rate of crystallization, G, defined as $G = 1/(t_{1/2})$, is obtained from the endotherm morphology of DSC analysis. The growth rate of crystallization can be expressed as follows according to the Hoffman and Lauritzen theory [19]:

$$G = G_0 \exp\left[-\frac{U^*}{R(T_c - T_\infty)}\right] \exp\left[-\frac{K_g}{T_c \Delta T f}\right] \tag{3}$$

where G_0 is a pre-exponential term, ΔT is equal to $T_m^0 - T_c$, R is the universal gas constant, U^* is the diffusional activation energy for the transport of crystallizable segments at the liquid–solid interface, and the recommended values $U^* = 6280$ J/mol [19]. T_c is the crystallization temperature, and T_∞ is the hypothetical temperature below which viscous flow ceases. Meanwhile, Hoffman et al. found $T_\infty = T_g - 30$ K; $f = 2T_c/(T_m^0 + T_c)$.

It is most convenient to rearrange Eq. (4) as follows:

$$\ln G + U^*/\left[R(T_c - T_\infty)\right] = \ln G_0 - K_g/(T_c \Delta T f) \tag{4}$$

According to Eq. (4), a plot of $\ln G + U^*/[R(T_c - T_\infty)]$ against $1/(T_c \Delta T f)$ should yield a straight line with an intercept $\ln G_0$ and a slope $-K_g$. The nucleation constant K_g is listed in Table 2. The K_g for the MRSF/HDPE composites are lower than those for pure HDPE.

The nucleation constant K_g contains contributions from the surface free energies, and it can be obtained from Eq. (5):

$$K_g = \frac{r b_0 \sigma \sigma_e T_m^0}{k \Delta H_m^0} \tag{5}$$

where σ and σ_e are the lateral and surface free energies of the growing crystal, respectively, the value of σ_e is 9.3×10^{-2} J/m^2, the recommended values $\Delta H_m^0 = 293$ J/g [20], and b_0 is the distance between two adjacent fold planes, taken to be the perpendicular separation of planes. This is 0.415 nm [20]. k is the Boltzmann constant, and r is a variable that considers the crystallization regime and assumes the value 4 for the regimes I and III, and the value 2 for the regime II. This is 4. According to Eq. (5), σ is obtained and listed in Table 2. As compared to pure HDPE, the decrease in σ indicates that the crystallization ability of MRSF/HDPE composites is lower than that of HDPE.

3.2. Non-isothermal crystallization kinetics of MRSF/HDPE composites

3.2.1. Theoretical background

Just like isothermal analysis, non-isothermal crystallization can also be analyzed by the Avrami equation, but considering the non-isothermal characterization of the process investigated and the effect of the cooling rate, Jeziorny [21] thought that was corrected by the cooling rate as follows:

$$\ln Z_c = \frac{\ln Z_t}{\phi} \tag{6}$$

where ϕ is the cooling rate, and Z_c is the kinetic crystallization rate constant.

Ozawa [22] extended the Avrami equation to the non-isothermal condition. Assuming that the nonisothermal crystallization process may be composed of infinitely small isothermal crystallization steps, the following equation was derived:

$$1 - X_t = \exp\left[-K(T)/\phi^m\right] \tag{7}$$

or

$$\ln\left[-\ln(1 - X_t)\right] = \ln K(T) - m \ln \phi \tag{8}$$

where $K(T)$ is the crystallization rate constant, X_t is the relative crystallinity, ϕ is the cooling rate, and m is the Ozawa exponent depending on the crystal growth and nucleation mechanism. According to Ozawa's theory, the relative crystallinity, X_t, can be calculated from these equations. By drawing the

Table 3
T_{onset}, T_{peak}, $t_{1/2}$, n, Z_c at different cooling rates

Samples	ϕ (°C/min)	T_{onset} (°C)	T_{peak} (°C)	ΔH_c (J/g)	$t_{1/2}$ (s)	n	Z_c
Neat HDPE	2.5	120.9	119.5	171.9	37	2.4	1.41
	5	119.8	118.0	166.2	24	2.3	1.44
	10	118.6	116.2	161.7	16	2.2	1.28
	15	118.4	114.9	158.9	15	2.3	1.23
HDPE/MRSF (100/20 w/w)	2.5	121.9	119.1	157.5	65	2.5	0.81
	5	120.8	117.1	153.3	46	2.5	0.94
	10	119.6	115.0	149.3	29	2.4	1.15
	15	118.5	112.5	147.4	26	2.2	1.11
HDPE/MRSF (100/40 w/w)	2.5	122.3	118.6	129.7	84	2.6	0.63
	5	120.8	116.4	129.6	51	2.4	1.01
	10	119.6	113.1	128.9	38	2.4	1.08
	15	118.3	110.7	122.8	29	2.3	1.09
HDPE/MRSF (100/60 w/w)	2.5	122.3	119.3	99.5	74	2.6	0.73
	5	121.3	117.4	97.7	47	2.5	1.06
	10	119.6	114.9	94.4	31	2.3	1.14
	15	118.3	112.9	86.6	28	2.3	1.10
HDPE/MRSF (100/80 w/w)	2.5	122.4	118.8	104.1	73	2.4	0.71
	5	121.2	116.6	97.5	49	2.3	1.02
	10	119.6	113.6	97.5	34	2.2	1.10
	15	118.3	111.7	94.6	28	2.2	1.09
HDPE/MRSF (100/100 w/w)	2.5	122.3	119.2	92.4	77	2.4	0.69
	5	121.3	117.2	88.9	50	2.3	1.02
	10	119.6	114.2	86.0	34	2.2	1.10
	15	118.3	110.8	81.8	31	2.2	1.08

plot of $\ln[-\ln(1-X_t)]$ versus $\log\phi$ at a given temperature, we should obtain a series of straight lines if the Ozawa analysis is valid, and the kinetic parameters m and $K(T)$ can be derived from the slope and the intercept, respectively.

A method modified by Mo was also employed to describe non-isothermal crystallization which combines the Avrami equation with the Ozawa equation. Its final form is given as follows [23]:

$$\ln\phi = \ln F(T) - \alpha \ln t \tag{9}$$

where the parameter $F(T) = [K(T)/Z_t]^{1/m}$, and $F(T)$ refers to the value of cooling rate chosen at unit crystallization time when the system amounted to a certain degree of crystallinity. The smaller the value of $F(T)$, the higher the crystallization rate. Therefore, $F(T)$ has a definite physical and practical meaning. Meanwhile, a refers to the ratio of the Avrami exponent n to the Ozawa exponent m ($a = n/m$). Plotting $\lg\phi$ versus $\ln t$ yields a linear relationship between $\lg\phi$ and $\ln t$. The data of kinetic parameter $F(T)$ and a can be estimated from the intercept and slope.

3.2.2. Non-isothermal crystallization behavior of HDPE and MRSF/ HDPE composites

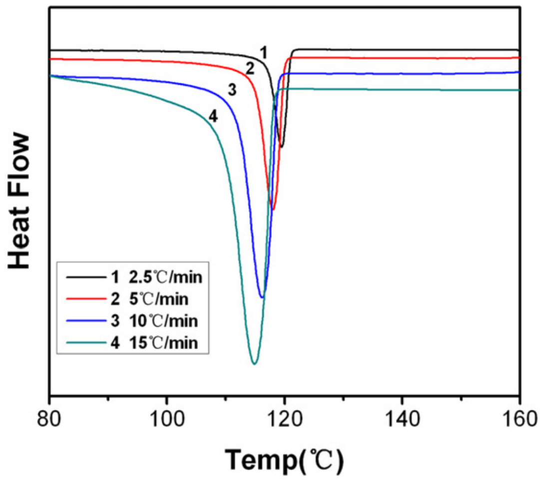

Fig. 4. Non-isothermal crystallization exotherms of the neat HDPE.

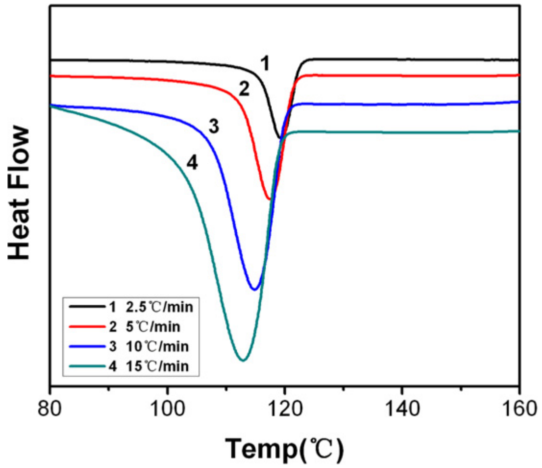

Fig. 5. Non-isothermal crystallization exotherms of the HDPE/MRSF composite (100/60 W/W).

The non-isothermal crystallization exotherms of the neat HDPE and MRSF/HDPE composites at four cooling rates of 2.5, 5, 10, and 15 °C/min are shown in Figs. 4 and 5. Some kinetic parameters can be derived from the DSC curves. They are the peak temperature, T_{peak}, the relative degree of crystallinity X_t, crystallization enthalpy ΔH_c, starting crystallization temperature T_{onset}, which is the temperature at the crossing point of the tangents of the baseline and the high temperature side of the exotherm, and the half crystallization time, $t_{1/2}$, which are listed in Table 3. The effect of the different cooling rates is as follows. The faster the cooling rate, the lower the temperature range at which the crystallization occurs, and at a slower cooling rate, there is sufficient time to activate nuclei at higher temperature. On the contrary, at faster cooling rates, the activation of the nuclei occurs at a lower temperature. $t_{1/2}$ showed that the crystallization rate of HDPE was higher than the MRSF/HDPE composites with given cooling rates, indicating that the MRSF cannot act as a nucleating agent for the HDPE matrix, and larger size of MRSF can lessen the adsorption of MRSF to HDPE chain due to steric hindrance. The peak temperature T_{peak} shifts to a lower temperature with an increasing cooling rate for both the neat HDPE and the MRSF/ HDPE composites. For a given cooling rate, the T_{peak} of the MRSF/ HDPE composites is slightly higher than that of the neat HDPE, indicating that the addition of MRSF into HDPE increases the crystallization rate of HDPE. The half crystallization time $t_{1/2}$ decreased with the increasing cooling rate. The crystallization enthalpy ΔH_c decreases as the cooling rate increases, but is shifted to lower values when the MRSF loading

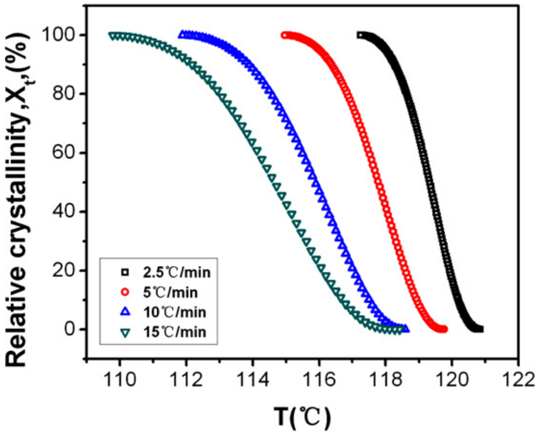

Fig. 6. Plots of X_t versus T for crystallization of the neat HDPE.

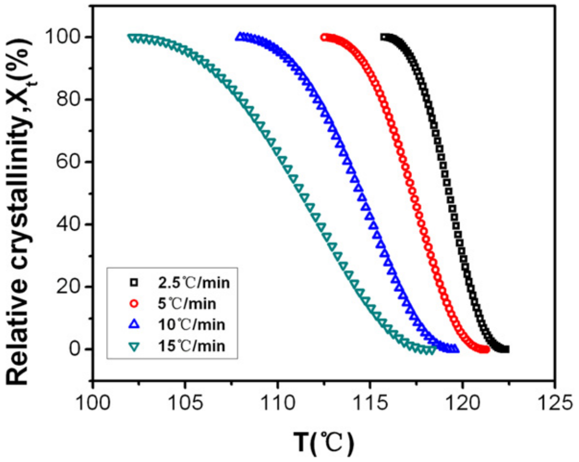

Fig. 7. Plots of X_t versus T for crystallization of the HDPE/MRSF composite (100/60 W/W).

in the composites increases. This means that the crystallization of MRSF/HDPE composites becomes more imperfect than that of the neat HDPE. The relative degree of crystallinity X_t is a function of temperature which is plotted in Figs. 6 and 7. It can be seen that all of the curves have the same reversed "S" shape. However, because of shorter crystallization time at a faster cooling rate, the values of X_t are lower than those that do at a slower cooling rate at the same crystallization temperatures.

3.2.3. *Avrami method*

The plots of $\ln[-\ln(1-X_t)]$ versus $\ln t$ for the non-isothermal crystallization of the neat HDPE and the MRSF/HDPE composites (100/60 W/W) at four cooling rates of 2.5, 5, 10, and 15 °C/min are shown in Figs. 8 and 9. A good linear relationship is shown. Two adjustable parameters, Z_t and n, can be obtained by linear regression. The Z_t and n parameters do not have the same physical meaning as in the isothermal crystallization because the temperature varies constantly in non-isothermal crystallization. This affects the rates of both nuclei formation and spherulite growth ascribed to their temperature dependence. Therefore, Z_t must be calibrated by the Jeziorny method. The reported values of n for polyethylene in the literature range from 2 to 4 (mostly for isothermal crystallization). The values reported by Rabesiaka and Kovacs [24] were in the range of 2.8–3.8. The results are listed in Table 3. As can be seen from the table, the simplified assumption that crystallization occurs under continuous temperatures is satisfied. That the range of the n value is 2–3 suggests that the non-isothermal crystallization of the neat HDPE and the MRSF/HDPE composites corresponds to a tridimensional growth with heterogeneous nucleation. The value of Z_c increases roughly while increasing the cooling rates for the neat HDPE and the MRSF/ HDPE composites.

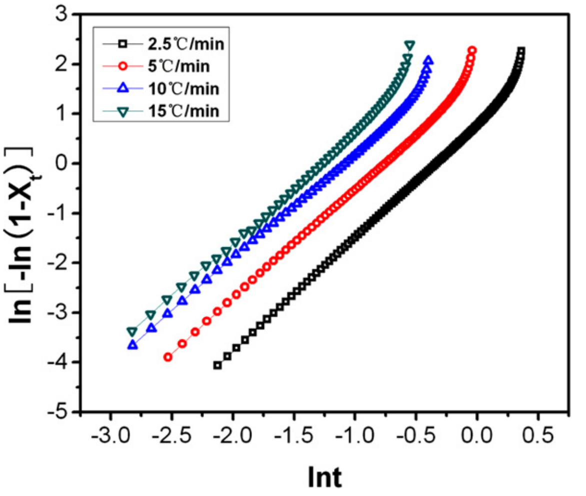

Fig. 8. Plots of $\ln[-\ln(1-X_t)]$ versus $\ln t$ for the non-isothermal crystallization of the neat HDPE.

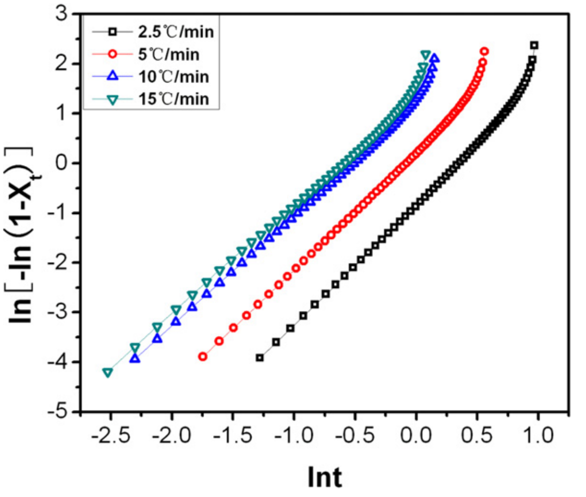

Fig. 9. Plots of $\ln[-\ln(1-X_t)]$ versus $\ln t$ for the non-isothermal crystallization of the HDPE/MRSF composite (100/60 W/W).

It is found that n displays a range of values, and decreases as the crystallization temperature decreases. This result is consistent with that of Eder and Wlochowicz's work [25]. At least two factors may affect the values of n. One factor is that the fast crystallization rate of HDPE at lower temperatures (higher supercoolings) prevents the spherulites from their full development. Thereby the value of n is lowered. Another one is that the growth site impingement, truncation of spherulites and secondary crystallization may change the crystallization mechanism. At higher crystalline volume fractions, the effects of impingement, truncation of spherulites and secondary crystallization become very important and decrease the overall crystallization rate. Finally, the value of n is reduced.

At a given crystallization temperature, the values of n for filled HDPE are lower than those for unfilled HDPE. It has been reported that organic and inorganic pigments might accelerate the non-isothermal and isothermal crystallization of HDPE and decrease the Avrami exponent. However, the presence of mineral fillers in HDPE melt does not change the type of nucleation and growth geometry. A possible explanation for the gradual decrease in the value of n at lower crystallization temperatures is that due to the non-isothermal nature of the experiment, the overall crystallization rate would increase as the decrease of temperature (higher supercooling). If nuclei are distributed in clusters (non-uniformly), then the impingement effect may occur. As a result, the values of n are reduced [26].

3.2.4. The Ozawa method

The non-linear dependence of $\ln[-\ln(1-X_t)]$ upon $\ln\phi$ shows that the Ozawa equation is not suitable to describe the non-isothermal crystallization in the neat HDPE and the MRSF/HDPE composite. For polyethylene and its composites, the crystallization is complicated due to an additional slow process, referred to as secondary crystallization, which is considered to involve the improvement of the crystalline order. The secondary crystallization effect for polyethylene may be due to the unfulfilled Ozawa equation.

3.2.5. The Mo method

The plots of the $\ln\phi$ versus $\ln t$ for the non-isothermal crystallization of the neat HDPE and the MRSF/HDPE composites at various relative crystallinities are shown in Figs. 10 and 11 from which the values of a and $F(T)$ can be obtained by the slopes and the intercepts of these lines, respectively (Table 4). It can be seen from Table 4 that the values of $F(T)$ systematically increase with an increase in the relative degree of crystallinity. At a given degree of crystallinity, the higher the $F(T)$ value, the higher the cooling rate needed within unit crystallization time, indicating the difficulty of polymer crystallization. By comparing the values of $F(T)$ of different samples, we have found that the values of neat HDPE are lower than those of composites, indicating that the crystallization rate of virgin HDPE is faster than that of MRSF/HDPE composites. This is in accordance with the result obtained from the Avrami approach.

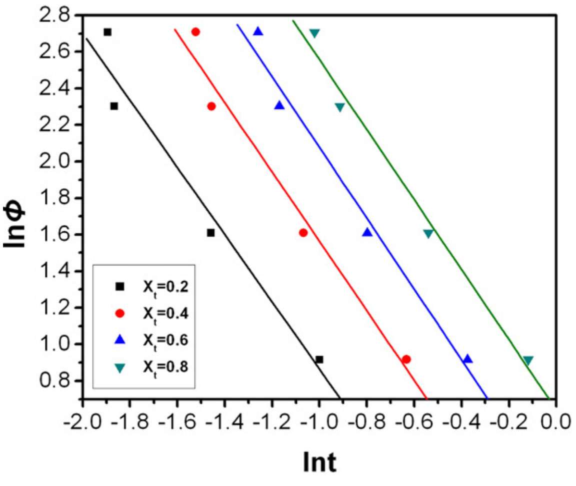

Fig. 10. Plots of the $\ln\phi$ versus $\ln t$ for the non-isothermal crystallization of the neat HDPE.

3.3. Morphological observation

Fig. 12 shows POM images of pure HDPE and four MRSF/HDPE composites with different sizes of RSF. In Fig. 12,

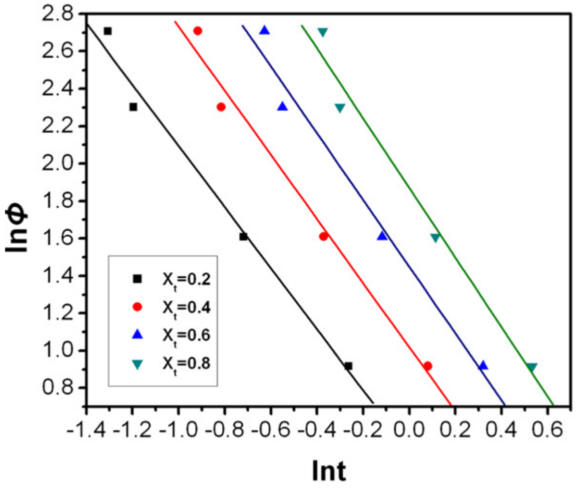

Fig. 11. Plots of the $\ln\phi$ versus $\ln t$ for the non-isothermal crystallization of the HDPE/MRSF composite (100/60 W/W).

Table 4
Non-isothermal crystallization kinetic parameters based on the Mo method

Samples	X_t	$F(T)$	α
Neat HDPE	0.2	0.38	1.84
	0.4	0.72	1.90
	0.6	1.15	1.94
	0.8	1.90	1.91
HDPE/RSF (100/20 w/w)	0.2	1.45	1.63
	0.4	2.41	1.75
	0.6	3.61	1.86
	0.8	5.49	1.94
HDPE/RSF (100/40 w/w)	0.2	2.01	1.63
	0.4	3.45	1.71
	0.6	5.13	1.78
	0.8	7.51	1.85
HDPE/RSF (100/60 w/w)	0.2	1.58	1.63
	0.4	2.77	1.71
	0.6	4.25	1.78
	0.8	6.49	1.86
HDPE/RSF (100/80 w/w)	0.2	1.55	1.72
	0.4	2.84	1.80
	0.6	4.44	1.86
	0.8	6.90	1.90
HDPE/RSF (100/100 w/w)	0.2	1.59	1.77
	0.4	2.97	1.84
	0.6	4.77	1.88
	0.8	7.44	1.93

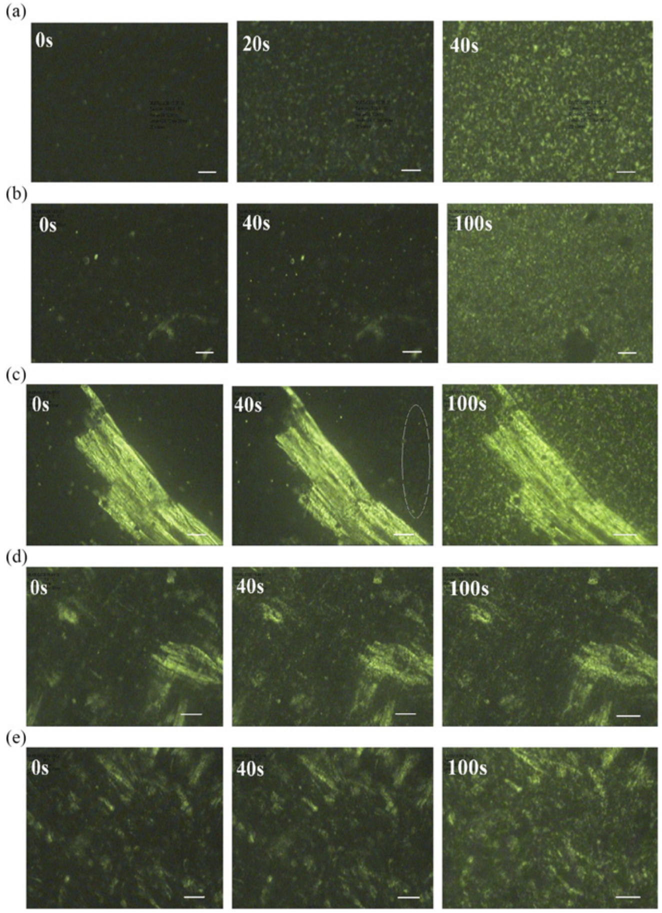

Fig. 12. Polarized optical micrographs at different time crystallizing at 123°C for: (a) neat HDPE; (b) HDPE:MRSF = 100:100 (by weight), size of RSF is 245 µm; (c) HDPE:MRSF = 100:100, size of RSF is 149 µm; (d) HDPE: MRSF = 100:100, size of RSF is 74 µm; (e) HDPE:MRSF = 100:100, size of RSF is 37 µm (all white bars in images are 10 µm).

volume filling spherulites can be seen for pure HDPE and the MRSF/HDPE composites (HDPE:MRSF = 100:100 by weight). As compared with pure HDPE, the smaller sizes of spherulites for four MRSF/HDPE 100/100 composites suggest that the MRSF cannot act as a nucleating agent for the HDPE matrix resulting as supported by DSC data. The reason can be that MRSF with big size of respective 245, 149, 74, 37 µm can be not nucleating centres and high ratio of MRSF and HDPE lessen the adsorption of MRSF to the HDPE chain and HDPE matrix is difficult to grow due to steric hindrance.

4. Conclusions

A systematic study of the isothermal and non-isothermal crystallization kinetics of the neat HDPE and the MRSF/HDPE composites has been performed by DSC.

For isothermal studies, as compared to the crystallization process of neat HDPE, the values of the Avrami exponent n of the MRSF/HDPE composites roughly increased. The $t_{1/2}$ values of the composites are higher than those of neat HDPE. This implies that MRSF decelerates the crystallization of HDPE in the composites. According to the Hoffman–Weeks theory, the values of the equilibrium melting point (T_m^0) increase with an increase in the content of MSRF in the composites. Moreover, according to the Hoffman theory, MRSF/HDPE composites had a lower lateral free energy of the growing crystal for crystallization than neat HDPE, which was related to the heterogeneous nucleation effect of MRSF.

For non-isothermal studies, the crystallization kinetics of each sample was investigated according to three various kinetic models, namely, the Avrami method, the Ozawa method, and the Mo method. The Avrami equation modified by Jeziorny's method and the Mo method are successful for describing the non-isothermal crystallization process of the neat HDPE and the MRSF/HDPE composites. Meanwhile, the Ozawa equation fails to provide an adequate description of non-isothermal crystallization. In the Avrami method, the parameters Z_c and $t_{1/2}$ suggest that for all samples, the rates of crystallization increase with an increase in cooling rate. The changes in the n value illustrate that the crystallization mechanism of the neat HDPE and the MRSF/HDPE composites is different. Particularly, $t_{1/2}$ showed that the crystallization rate of HDPE was higher than that of the MRSF/ HDPE composites with given cooling rates.

Acknowledgements

Contract grant sponsor: National High Technology Research and Development Program of China (863 Program); contract grant number: 2002AA6Z3181.

References

[1] Z.H. Liu, K.W. Kwok, R.K.Y. Li, C.L. Choy, Effects of coupling agent and morphology on the impact strength of high density polyethylene/$CaCO_3$ composites, Polymer 43 (2002) 2501–2506.

[2] A. Gungor, The physical and mechanical properties of polymer composites filled with Fe powder, J. Appl. Polym. Sci. 99 (2006) 2438–2442.

[3] M. Zhang, P.F. Fang, S.P. Zhang, B. Wang, S.J. Wang, Study of structural characteristics of HDPE/$CaCO_3$ nanocomposites by positrons, Radiat. Phys. Chem. 68 (2003) 565–567.

[4] B. Magnus, O. Kristuuna, The use of silane technology in crosslinking polyethylene/wood flour composites, Compos. Part A: Appl. Sci. 37 (2006) 752–765.

[5] J.Z. Lu, I.I. Negulescu, Q.L. Wu, Maleated wood-fiber/high-density-polyethylene composites: Coupling mechanisms and interfacial characterization, Compos. Interface 12 (2005) 125–140.

[6] P.J. Herrera-Franco, A. Valadez-Gonzalez, Mechanical properties of continuous natural fibre-reinforced polymer composites, Compos. Part A: Appl. Sci. 35 (2004) 339–345.

[7] S. Panthapulakkal, S. Law, M. Sain, Enhancement of processability of rice husk filled high-density polyethylene composite profiles, J. Thermoplast. Compos. 18 (2005) 445–458.

[8] P.P. Kundu, J. Biswas, H. Kim, S. Choe, Influence of film preparation procedures on the crystallinity, morphology and mechanical properties of LLDPE films, Eur. Polym. J. 39 (2003) 1585–1593.

[9] J.L. Chen, Q. Sun, Y.K. Zou, G. Xue, DSC studies on the melting crystallization of polyethylenes prepared from alkanes of varying molecular size, Polymer 43 (2002) 6887–6891.

[10] P.E. Kristiansen, E.W. Hansen, B. Pedersen, Isothermal crystallization of polyethylene monitored by in situ NMR and analyzed within the 'Avrami' model framework, Polymer 42 (2001) 1969–1980.

[11] G.D. Liang, J.T. Xu, W.B. Xu, PE/PE-g-MAH/Org-MMT nanocomposites. II. Nonisothermal crystallization kinetics, J. Appl. Polym. Sci. 91 (2004) 3054–3059.

[12] J.G. Gao, D. Wang, M.S. Yu, Z.H. Yao, Nonisothermal crystallization, melting behavior, and morphology of polypropylene/metallocene-catalyzed polyethylene blends, J. Appl. Polym. Sci. 93 (2004) 1203–1210.

[13] Q. Zheng, M. Peng, X.S. Yi, Crystallization of high density polyethylene: Effect of contact with NdFeB magnetic powder substrates, Mater. Lett. 40 (1999) 91–95.

[14] M.T. Run, J.G. Gao, Z.T. Li, Nonisothermal crystallization and melting behavior of mPE/LLDPE/LDPE ternary blends, Thermochim. Acta 429 (2005) 171–178.

[15] M. Avrami, Kinetics of phase change. I. General theory, J. Chem. Phys. 7 (1939) 1103.

[16] M. Avrami, Kinetics of phase change. II. Transformation-time relations for random distribution of nuclei, J. Chem. Phys. 8 (1940) 212.

[17] M. Avrami, Granulation, phase change, and microstructure kinetics of phase change. III, J. Chem. Phys. 9 (1941) 177–184.

[18] J.D. Hoffman, J.J. Weeks, Melting process and the equilibrium melting temperature of polychlorotrifluoroethylene, J. Res. Natl. Bur. Stand. A 66 (1962) 13–18.

[19] J.D. Hoffman, G.T. Davis, S.I. Lauritzen, in: N.B. Hannay (Ed.), Treatise on Solid State Chemistry, Plenum, New York, 1976.

[20] M. Li, X.F. He, J.J. Liu, X.Q. Zhang, G. Sun, H.G. Cai, C.Y. Zhang, Crystallization behavior of polyethylene/ontmorillonite (MMT) nanocomposites by in situ polymerization, Chem. J. Chinese Univ. 7 (2006) 779–783.

[21] A. Jeziorny, Parameters characterizing the kinetics of the non-isothermal crystallization of poly (ethylene terephthalate) determined by d.s.c, Polymer 19 (1978) 1142–1144.

[22] T. Ozawa, Kinetics of non-isothermal crystallization, Polymer 12 (1971) 150–158.

[23] T.X. Liu, Z.S. Mo, S. Wang, H.F. Zhang, Nonisothermal melt and cold crystallization kinetics of poly(aryl ether ether ketone ketone), Polym. Eng. Sci. 37 (1997) 568–575.

[24] J. Rabesiaka, A.J. Kovacs, Isothermal crystallization kinetics of polyethylene. III. Influence of the sample preparation, J. Appl. Phys. 32 (1961) 2314–2320.

[25] M. Eder, A. Wlochowicz, Kinetics of non-isothermal crystallization of polyethylene and polypropylene, Polymer 24 (1983) 1593–1595.

[26] L.C. Lopez, G.L. Wilkes, Non-isothermal crystallization kinetics of poly(p-phenylene sulphide), Polymer 30 (1989) 882–887.